Shear-flexural strength mechanical model for the design and assessment of reinforced concrete beams subjected to point or distributed loads

Running title (*short title version up to 80 characters including space)*: Shear-flexural strength model for RC beams with point or distributed loads.

Antonio Marí[1], Antoni Cladera[2], Jesús Bairán[1], Eva Oller[1] and Carlos Ribas[2]

(1) *Department of Construction Engineering, Universitat Politècnica de Catalunya, Barcelona, Spain*

(2) *Department of Physics. University of Balearic Islands, Palma de Mallorca, Spain*

Corresponding author: Antonio Marí, Department of Construction Engineering, Universitat Politècnica de Catalunya, c/Jordi Girona 1-3 C1 201 08034 Barcelona, Spain. Phone number: +34 93 401 65 08. E-mail:antonio.mari@upc.edu

Abstract:

A mechanical model recently developed for the shear strength of slender reinforced concrete beams with and without shear reinforcement is presented and extended to elements with uniformly distributed loads, specially focusing on practical design and assessment in this paper. The shear strength is considered to be the sum of the shear transferred by the concrete compression chord, along the crack, due to residual tensile and frictional stresses, by the stirrups and, if they exist, by the longitudinal reinforcement. Based on the principles of structural mechanics simple expressions have been derived separately for each shear transfer action and for their interaction at ultimate limit state. The predictions of the model have been compared to those obtained by using the EC2, MC2010 and ACI 318-08 provisions and they fit very well the available experimental results from the recently published ACI-DAfStb databases of shear tests on slender reinforced concrete beams with and without stirrups. Finally, a detailed application example has been presented, obtaining each contributing

component to the shear strength and the assumed shape and position of the critical crack.

Keywords: Shear strength, mechanical model, reinforced concrete, design, assessment, shear tests.

Notations

a	shear span
b	width of concrete section
d	effective depth to main tension reinforcement
d_{max}	maximum aggregate size
f_{ck}	characteristic value of the cylinder concrete compressive strength
f_{cm}	mean value of the cylinder concrete compressive strength
f_{ct}	uniaxial concrete tensile strength
f_{ctm}	mean value of the concrete tensile strength
f_{yw}	yield strength of the transverse reinforcement
h	overall depth of concrete section
s	longitudinal coordinate from the support
s_{cr}	location of the section where the critical shear crack starts
s_{mx}	average crack spacing of inclined cracks along the beam axis
$s_{m\theta}$	average crack spacing of inclined cracks
s_{u}	location of the shear critical section
v_c	dimensionless contribution to the shear strength of the un-cracked concrete chord
v_l	dimensionless contribution to the shear strength of the longitudinal reinforcement.
v_s	dimensionless contribution to the shear strength of the transverse reinforcement
v_u	dimensionless ultimate shear force
$v_{u,0}$	dimensionless ultimate shear force of beams and one-way slabs without transverse reinforcement
v_w	dimensionless shear force resisted along the crack
x	neutral axis depth
x_w	vertical projection of length along the crack where the tensile stresses are extended
z	lever arm
A_s	longitudinal reinforcement area
A_{sw}	area per unit length of the transverse reinforcement
C	compression force in the un-cracked concrete chord
E_c	modulus of elasticity of concrete
E_s	modulus of elasticity of steel
G_f	concrete fracture energy
K_λ	constant

M	bending moment
M_{cr}	cracking moment
R_t	ratio between the principal tensile stress and the tensile strength
T	tensile force in the longitudinal reinforcement
V	shear force
V_c	contribution to the shear strength of the un-cracked concrete chord
V_l	contribution to the shear strength of the longitudinal reinforcement
V_{pred}	predicted value of the ultimate shear force
V_s	contribution to the shear strength of the transverse reinforcement
V_{Sd}	design shear force
V_{test}	experimental value of the ultimate shear force
V_u	ultimate shear force
$V_{u,0}$	ultimate shear force of beams and one-way slabs without transverse reinforcement
V_w	shear force resisted along the crack
α_e	modular ratio (E_s/E_c)
$\varepsilon_{ct,cr}$	concrete strain at the beginning of macro-cracking
$\varepsilon_{ct,u}$	ultimate tensile strain
ε_s	strain at the longitudinal reinforcement
ζ	size effect factor
λ	distance from the neutral axis
θ	inclination angle of the strut
ρ	longitudinal tension reinforcement ratio
ρ_w	transverse reinforcement ratio
σ_1, σ_2	principal stresses
σ_x	normal stress in the longitudinal direction
σ_y	normal stress in the transverse direction
σ_w	normal stress in a horizontal fiber in the cracked web

1. INTRODUCTION

Shear strength verification and design of slender reinforced concrete (RC) elements is still an intensive research topic. When a RC element is subjected to a combination of shear and flexure, diagonal cracks appear and multi-axial stress states take place in regions that exhibit a markedly complex behavior, resulting the so-called shear resisting actions. These shear resisting actions contribute to the shear force transfer between the two portions of the element at each side of the crack. It is well-accepted that the following shear resisting actions exist: shear resisted in the un-cracked compression chord of the beam, shear transferred in the cracked zone of the element by means of aggregate interlock and softening residual tensile stresses, dowel action of the longitudinal reinforcement and the truss action requiring transversal reinforcement.

The mechanics of the previous actions is very diverse and exhibits complex interaction among them; hence development of a universally accepted formulation to account for shear forces has not been achieved yet. On the other hand, design approaches in most current codes of practice are empirically or semi-empirically based and show large scatter with respect to experimental evidence; thus, large safety factors are needed to assure their safe applicability. Recently, it has been suggested in Mari et al. [1] that the fact that most of empirical formulations explicitly or implicitly assume prevailing of one of the above mentioned actions, implies that such type of formulation can only partially explain the phenomenon, being this a plausible explanation of the big dispersion.

In the last decades, refined numerical models capable to capture the complex observed shear behavior have been developed. Some examples are [2-10], among others. A review of the basis of non-linear cross-section analysis with tangential stresses can be found in [11]. These developments are complex for daily practice and do not substitute conceptual hand procedures; however, they have contributed to the assessment of structures and have complemented experimental observation to better understand the role and evolution of the different resisting actions.

Transfer of the previous knowledge to the development of rational design formulations is of paramount importance, as current design practice and codes tend more to performance-based-design basis. Currently, large databases compiling shear

experiments have been developed by Reineck et al. [12, 13] in the context of an ACI-DAfStb joint group, resulting in a powerful tool for evaluating the adequacy of different formulations to reproduce the role of the design variables. In this paper, the rational shear resistance formulation of Mari et al [1] is briefly presented and evaluated against the latest databases [12, 13]. One significant characteristic of the proposed formulation is that most important shear transfer actions are separately considered. In this paper, the influence of the different design variables are evaluated against experimental observations and compared with other code design formulations. In general, the proposed formulation has less dispersion than other approaches, smaller mean error and produces results in the safe side. Moreover, in this paper the extension of the proposed method to elements with distributed loads is carried out. Finally, a detailed work example is presented to show the easiness of use of the proposed formulation.

2. MECHANICAL MODEL FOR SHEAR CAPACITY OF SLENDER RC ELEMENTS

Fig. 1 depicts the sequence of crack propagation of the typical slender element without stirrups failing in shear. In Fig. 1a, it can be observed that, at a certain load level before failure, the width of the critical shear crack in the web is moderate and shear transfer across it, in terms of aggregate interlock and residual tensile strength, is expected to be the most relevant part of concrete shear contribution. At subsequent loading, crack width in the web considerably increases, thus shear resistance in the cracked web softens and reduces its contribution where crack widths are bigger. Moreover, the formation of a new crack branch in the compression zone of the beam is evident at a slightly higher position than the tip of the web's crack, resulting from the combination of shear and compression stresses in the compression chord (Figs. 1b and 1c); this crack denotes an increment of shear resisted in the compression chord. Ultimate failure of the element takes place when reaching the capacity of the compression head under multi-axial loading, Fig. 1d.

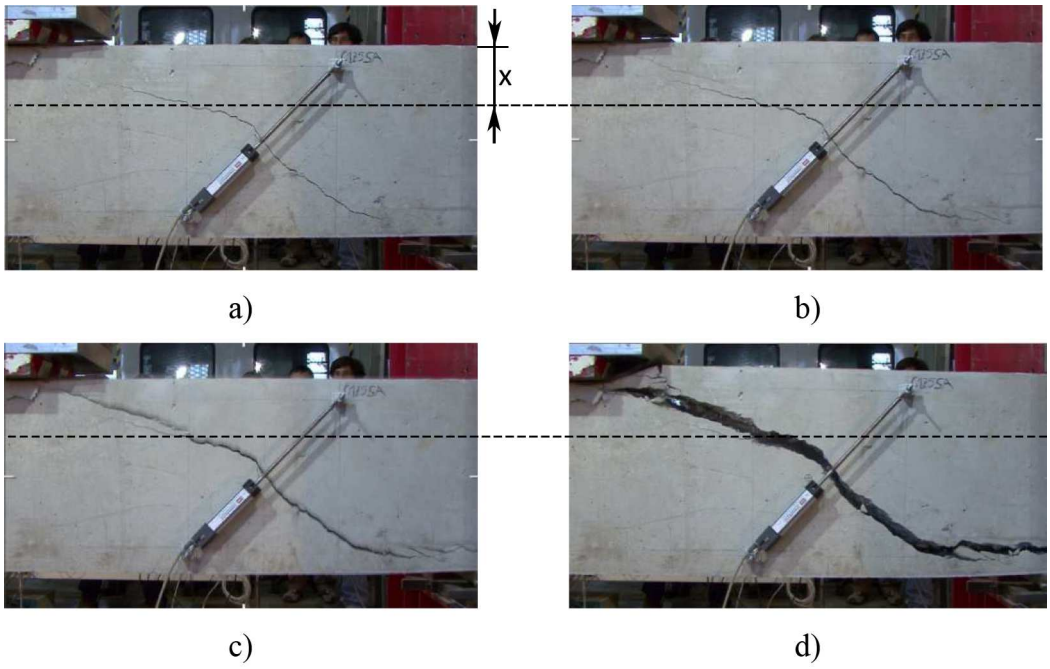

Figure 1. Sequence of cracking evolution in a shear failing element. Adapted from [1].

As widely accepted, the total shear resistance, Eq. 1, is considered to be the combination of the shear resisted by concrete and by the transverse reinforcement (V_s). However, the shear resistant contribution of concrete is explicitly separated into the following components, whose importance are considered to be variable as damage propagates: shear resisted in the uncrack compression head (V_c), shear transfer across web cracks (V_w) and the contribution of the longitudinal reinforcement (V_l). It should be highlighted that here V_c represents the contribution of shear in the compression chord of the beam, not the total concrete contribution to shear.

$$V = V_c + V_w + V_l + V_s = f_{ct} \cdot b \cdot d \cdot \left(v_c + v_w + v_l + v_s \right) \tag{1}$$

where v_c, v_w, v_l and v_s are the dimensionless values of the shear transfer actions. All these components play a role in the shear resisting mechanics along the different load stages. As the load increases, the crack with increases and the aggregate interlock decreases; therefore, due to equilibrium, the decrease on aggregate interlock must be balanced by an increase in the shear transferred by the compression concrete chord. Hence, in the limit state, previous to incipient failure (between Figs. 1c and 1d), the shear stress distribution in the critical section is assumed to be similar to the one represented in Fig. 2; where the approximated distribution of each contributing action is

also indicated, *x* is the neutral axis and *d* the effective depth of the section. This stress profile is a qualitative distribution of the stresses in a section close to that of the tip of the first branch of the critical crack and it is not affected by the local state of stresses around the tip.

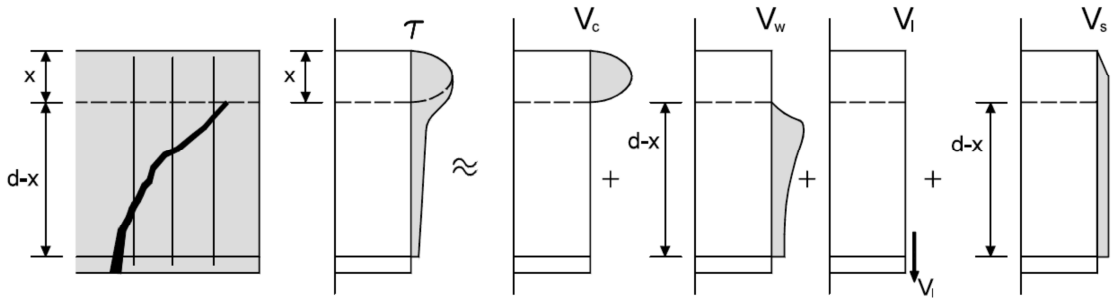

Figure 2. Distribution of shear stresses in the imminent failure situation and qualitative distribution of the different contributing actions

The following additional simplifications are also considered:

1. Neutral axis (*x*) depth and height of un-cracked zone are treated as equivalent. It is assumed that it can be obtained by standard analysis of cracked reinforced concrete sections under pure flexure. For sections without compressive reinforcement the expression of the neutral axis depth is given by Eq. (2).

$$\xi = \frac{x}{d} = \alpha_e \cdot \rho \cdot \left(-1 + \sqrt{1 + \frac{2}{\alpha_e \cdot \rho}} \right) \tag{2}$$

   where $\alpha_e = E_s/E_c$ is the modular ratio between steel and concrete and $\rho = A_s/(b \cdot d)$ is the longitudinal reinforcement ratio , being *b* the section width. If compressive reinforcement is added, *x/d* would decrease. However, the compressive reinforcement contribution should be added and the steel can resist higher shear stresses compared to concrete. Therefore, in a conservative way, the compressive reinforcement is neglected in the model.
2. Based on experimental and numerical observations, crack inclination is approximated as in Eq. (3). This is equivalent to considering the horizontal projection of the first branch of the flexural-shear critical crack equals 0.85*d*.

$$\cot\theta = \frac{0.85}{1-\frac{x}{d}} \quad (3)$$

This value is in accordance with experimental observations made by the authors [14-17]. In any case, the inclination of the cracks is affected by the longitudinal and transverse reinforcement ratios ρ and ρ_w, respectively, which influence the strains state. However, as observed by other researchers [18], in general this influence is moderate, being the effect of longitudinal reinforcement ratio more important [19]. Therefore, although the angle of the compression struts change, the horizontal projection of the critical shear crack does not change as much, since the increment of longitudinal reinforcement ratio increases and neutral axis depth, *x*.

3. The weakest section in front of a combined shear-bending failure is considered to be placed at the tip of the first branch of the critical crack for beams with constant geometry and reinforcement (Fig. 3). Any other section closer to the zero bending moment point has a bigger depth of the compression chord, produced by the inclination of the crack and will resist a bigger shear force. Any other section placed farther from the support will have the same depth of the compression chord but will be subjected to higher normal stresses and, therefore, will have a higher shear transfer capacity. The critical crack (Fig. 3) is assumed to start where the bending moment diagram at failure reaches the cracking moment of the section, $s_{cr} = M_{cr}/V_u$, which is a conservative assumption.
4. Longitudinal reinforcement is in elastic regime; thus, horizontal normal stresses (σ_x) are computed according to linear theory.
5. When stirrups are anchored in the compression zone, they collaborate in the strength of the compression head by producing a confining vertical compression (σ_y) at depth larger than the concrete cover (*d'*).
6. Resistance of compression head is governed by Kupfer's biaxial failure envelope. It is considered that failure occurs when the principal stresses reach the Kupfer's compression-tension branch of the failure surface [20].

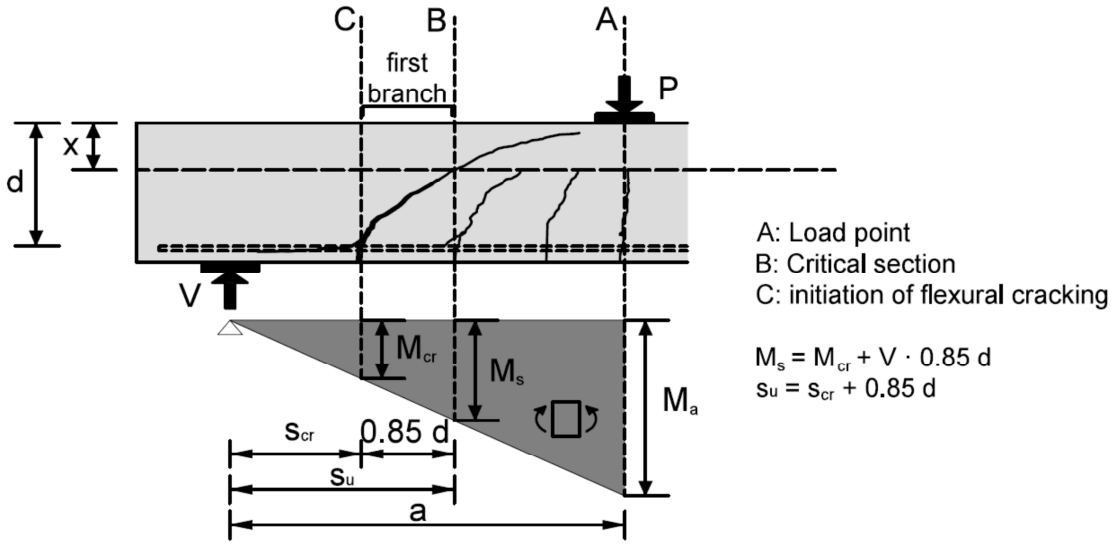

Figure 3. Position of the shear critical section in the beam

With the above considerations, the magnitude of each dimensionless contributing component at the imminent failure can be estimated as presented in Table 1. The development of the different equations is summarized in the following sections.

Contributing component	Final simplified dimensionless expressions	
Cracked concrete web	$v_w = 167\frac{f_{ct}}{E_c}\left(1+\frac{2E_cG_f}{{f_{ct}}^2 d}\right)$	(4)
Longitudinal reinforcement	$v_s > 0 \rightarrow \mathrm{v_l} = 0.25\frac{\mathrm{x}}{\mathrm{d}} - 0.05$	(5a)
	$v_s = 0 \rightarrow v_l = 0$	(5b)
Transversal reinforcement	$v_s = 0.85\rho_w\frac{f_{yw}}{f_{ct}}$	(6)
Compression chord	$v_c = \zeta\left[(0.88+0.70v_s)\frac{x}{d}+0.02\right]$	(7)
	$\zeta = 1.2 - 0.2\cdot a \geq 0.65 \quad (a\ in\ meters)$	(8)

Table 1. Summary of simplified expressions of dimensionless shear contributing components

The tensile concrete strength, f_{ct}, is evaluated in the application of the previous equations by using EC-2 equations, as shown in Eqs. (9-10), but limiting the concrete compressive strength to 60 MPa for the elements without stirrups, as it has been previously shown that the shear strength of reinforced concrete beams without stirrups does not increase significantly for high-strength concrete beams due to the fracture of the aggregates [14, 15]. For the test comparison carried out later in this paper, the mean concrete compressive strength, f_{cm}, has been used in Eq. (9) instead the characteristic value, f_{ck}. The concrete modulus of elasticity has also been evaluated according to EC-2, see Eq. (11).

$$f_{ctm} = 0.30 \cdot \sqrt[3]{f_{ck}^2} \quad if \ f_{ck} \le 60\, N/mm^2 \tag{9}$$

$$f_{ctm} = 2.12 \cdot \ln\left(1 + \frac{f_{cm}}{10}\right) \quad if \ f_{ck} > 60\, N/mm^2 \tag{10}$$

$$E_c = 22 \cdot \left(\frac{f_{cm}}{10}\right)^{0.3} \tag{11}$$

The fracture energy, G_f, is another important parameter of the model and it depends primarily on the water-cement ratio, the aggregate type, the maximum aggregate size, the age of concrete and the curing conditions. Equation (12) has been used to evaluate it. For more information about this equation, or the exact development of any of the contributing components, refer to [1].

$$G_f = 0.028 \cdot f_{cm}^{0.18} \cdot d_{\max}^{0.32} \tag{12}$$

One important characteristic of the presented model is that it could be directly extended to other types of concretes (i.e. self-consolidating concrete, huge fly ash replacements, fiber reinforced concrete) taking into account its correct mechanical properties [21-23].

2.1. Cracked concrete web contribution (v_w)

Shear resistance of cracked concrete in the web is considered as the residual tensile stress of cracked concrete. The mean tensile stress of the softening curve is considered distributed in a depth x_w of the cracked zone of the cross-section where the tensile σ-ε curve reaches zero tension, see Fig. 4. A linear softening branch of the σ-ε curve has been assumed which is consistently dependent on the fracture energy in mode I (G_f). The derivation of the equation is carried out in [1] and the resulting equation is presented in Eq. (4) of Table 1.

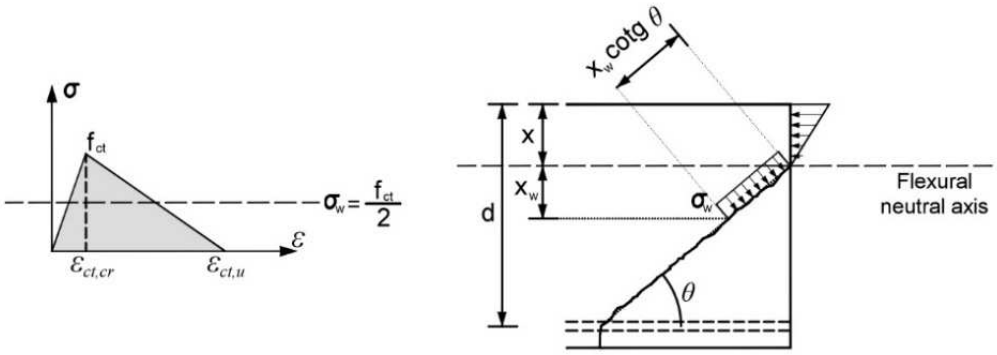

Figure 4. Contribution of cracked concrete to shear resistance

2.2. Longitudinal reinforcement contribution (v_l)

Contribution of longitudinal reinforcement, or dowel action, is considered only when transversal reinforcement exists, Eq. (5a), being negligibly when there are no stirrups, Eq. (5b). Stirrups provide a constraint to the vertical movement of the longitudinal bars, enabling them to transfer a certain shear. In order to evaluate such shear force, it is considered that the longitudinal bars are doubly fixed at the two stirrups adjacent to the crack initiation, and subjected to bending due to a relative imposed displacement between those points. This vertical relative displacement is caused by the critical crack opening and the shear deformation of the compression chord. This contributing component clearly depends on the tensile steel ratio which is implicitly represented by means of the *x/d* parameter. The simplified expression is presented in Eq. (5a) of Table 1.

2.3. Transversal reinforcement contribution (v_s)

Contribution of transversal reinforcement, Eq. (6) of Table 1, is taken as the integration of the stresses cut by the inclined crack up to a height of (*d*-*x*), see Fig. 2, and assuming that transversal reinforcement is yielded along the total crack height.

2.4. Compression head contribution (v_c)

The shear capacity of the compression chord is evaluated assuming that failure occurs when the first fiber in the compression chord reaches the Kupfer's failure envelope. By

means of a Mohr's circle analysis, Eq. (13) can be derived where σ_x is the normal stress in the most critical fiber, located at position $\lambda \cdot d$ from the bottom of the neutral axis. K_λ is a parameter relating the mean shear stress in the compression chord with stress in the critical fiber; therefore, it depends on the shape of the distribution of shear stresses in the compression chord (Fig. 2), and the critical fiber.

$$v_c = \frac{1}{f_{ct}} \zeta K_\lambda \frac{x}{d} \sigma_1 \sqrt{1 - \frac{(\sigma_x + \sigma_y)}{\sigma_1} + \frac{(\sigma_x \sigma_y)}{{\sigma_1}^2}} \tag{13}$$

Where ζ is the size effect parameter for the compression head (Eq. 8), which can be assimilated to that of a splitting test, as proposed by Zararis and Papadakis [24].

After a numerical parametric study, it was observed that the position of the critical fiber can be reasonably considered constant, for reinforced elements, as $\lambda \approx 0.45$. Therefore, the simplified shear stress distribution assumed in the concrete compressed head (see Fig. 2) barely affects its strength under a multiaxial state of stresses.

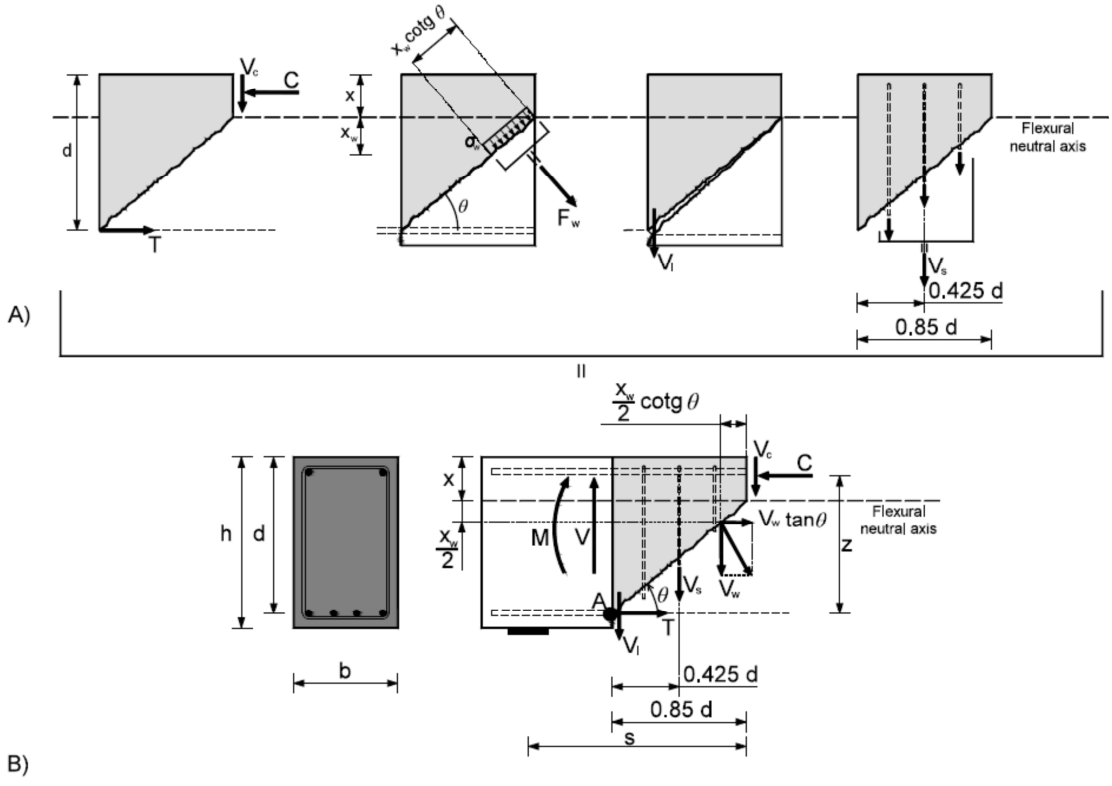

Figure 5. Shear transfer mechanisms considered

In order to obtain the beam strength, the shear capacity must be calculated at the critical section, placed at the tip of the first branch of the critical shear crack. Equilibrium between the internal forces (V, M) and the stress resultants (Fig. 5A) at the concrete chord (C, V_c) along the crack (V_w), at the stirrups (V_s) and at the longitudinal reinforcement (T, V_l) is taken in the portion indicated by Fig. 5B. Equilibrium of moments is taken with respect to the point A (Fig. 5B), where the critical crack reaches the reinforcement.

$$C = T + V_w \cdot \tan\theta \tag{14}$$

$$V = V_c + V_w + V_l + V_s \tag{15}$$

$$C \cdot z = M + V_c \cdot 0.85 \cdot d + V_w \cdot z_w + 0.5 \cdot V_s \cdot 0.85 \cdot d \tag{16}$$

where V_w is the vertical component of the tensile force transferred along the crack, and z_w is its lever arm with respect to point A

$$z_w = \frac{0.85 \cdot d - 0.5 \cdot x_w \cdot \cot\theta}{\cos^2\theta} \tag{17}$$

Further, by relating the vertical confining stress (σ_y) with the capacity of the transversal reinforcement (v_s), Eq. 18 is derived for the shear capacity of the compression chord, where $R_t = \sigma_1/f_{ct,}$ which is an implicit dependency on the applied bending moment.

$$v_c = R_t K_\lambda \zeta \frac{x}{d} \sqrt{1 - \frac{\lambda(0.4 + 1.7 v_c + 2 v_w z_w + 0.85 v_s)}{\frac{x}{d}\left(1 - \frac{x}{3d}\right) R_t} \left(\frac{v_s}{0.85 R_t} - 1\right) - \frac{v_s}{0.85 R_t}} \tag{18}$$

Equation 18 is a general expression based on a rational mechanical analysis; however, as can be observed, it is a recurrent equation on v_c which can be solved iteratively. However, it was found that the exact solution of Eq. (18), represented in Fig.6, can be very well approximated by the simplified linear equation presented in Eq. (7) of Table 1, in which the applied bending moment at the critical crack initiation was conservatively considered as the cracking moment. This approximate solution is represented in Fig. 6 with dashed lines. It is practically exact for beams without stirrups (v_s = 0) and to some extent conservative for shear reinforced members. It is observed that the shear transferred by the un-cracked concrete chord depends linearly on the neutral axis depth, as previously obtained in [25] using a similar approach. Since the

neutral axis depth depends on the longitudinal reinforcement ratio, ρ, and on the modular ratio, $\alpha_e = E_s/E_c$, the higher the longitudinal reinforcement amount, the higher the shear resisted by the concrete chord. In addition, it is observed that v_c depends also on the shear carried by the transverse reinforcement, v_s, as was observed experimentally [14, 26].

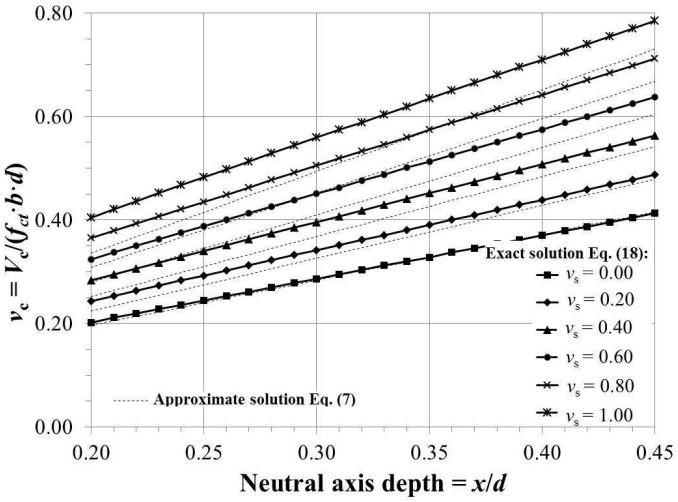

Figure 6. Contribution of un-cracked concrete chord to shear resistance

3. TRANSVERSE REINFORCEMENT DESIGN EQUATIONS

When the design shear force, V_{Sd}, exceeds the shear which the beam can resist without transverse reinforcement the amount of transverse reinforcement necessary to resist the design shear force must be obtained.

The total shear resisted by a beam without transverse reinforcement, $V_{u,0}$, will be that given by Eqs. (1) and (4)-(5b) and (7), making $v_s = 0$, resulting:

$$v_{u,0} = \frac{V_{u,0}}{f_{ct} \cdot b \cdot d} = v_c + v_w \tag{19}$$

$$V_{u,0} = f_{ct} \cdot b \cdot d \cdot v_{u,0} \tag{20}$$

When stirrups are added, V_l becomes a non-negligible contribution, and the amount of transverse reinforcement necessary to resist the difference V_{sd} - $(V_{u,0} + V_l)$ can be

obtained in dimensionless form by Eq. (21). This is a direct design equation, derived from the previous equations, and does not require iterations to obtain v_s.

$$If\ v_{Sd} > v_{u,0}\ ;\quad v_s = \frac{v_{Sd} - \zeta \cdot \left(0.88 \cdot \frac{x}{d} + 0.02\right) - v_w - v_l}{1 + 0.70 \cdot \zeta \cdot \frac{x}{d}} = \frac{v_{Sd} - \left(v_{u,0} + v_l\right)}{1 + 0.70 \cdot \zeta \cdot \frac{x}{d}} \tag{21}$$

where v_{sd} is the dimensionless design shear force, $v_{sd} = V_{sd}/f_{ct} \cdot b \cdot d$, which is a data of the problem.

4. BEAMS SUBJECTED TO UNIFORMLY DISTRIBUTED LOADS

In the case of beams subjected to uniformly distributed loads, the model can be applied taking into account that the shear force law diminishes with the distance from the support. Therefore, the critical shear crack will be even closer to the support in comparison to the case of a point load, as observed in the results of the Stuttgart tests [27] shown in Fig. 7. The effect of the uniform load can be considered including this type of load, q, in the equilibrium equations of the beam area affected by the critical crack:

$$C = T + V_w \cdot \tan\theta \tag{22}$$

$$V = V_c + V_w + V_l + V_s + q \cdot 0.85 \cdot d \tag{23}$$

$$C \cdot z = M + V_c \cdot 0.85 \cdot d + V_w \, z_w + 0.5 V_s \cdot 0.85 d + 0.5 q \cdot \left(0.85 d\right)^2 \tag{24}$$

$$v_c = R_t K_\lambda \zeta \frac{x}{d} \sqrt{1 - \frac{\lambda\left(0.4 + 1.7 v_c + 2 v_w z_w + 0.85 v_s + \frac{q}{f_{ct} \cdot b} \cdot 0.85^2\right)}{\frac{x}{d}\left(1 - \frac{x}{3d}\right) R_t} \left(\frac{v_s}{0.85 R_t} - 1\right)} - \frac{v_s}{0.85 R_t} \tag{25}$$

The effect of the uniformly distributed load may be easily seen by comparing Eqs. (22)-(25) with Eqs. (14)-(18). In the case of distributed load, the dimensionless compression chord shear strength will be given by Eq. (25) where the term that includes the uniform load ($\frac{q}{f_{ct} \cdot b} \cdot 0.85^2$) is negligible. Then, the concrete chord contribution V_c can be considered equal to that obtained in the case of point loads. However, the calculated value of the ultimate shear force corresponds to the critical section. So, the support reaction should

be obtained from this ultimate shear force, adding the resultant of the uniform load between this critical shear section and the support.

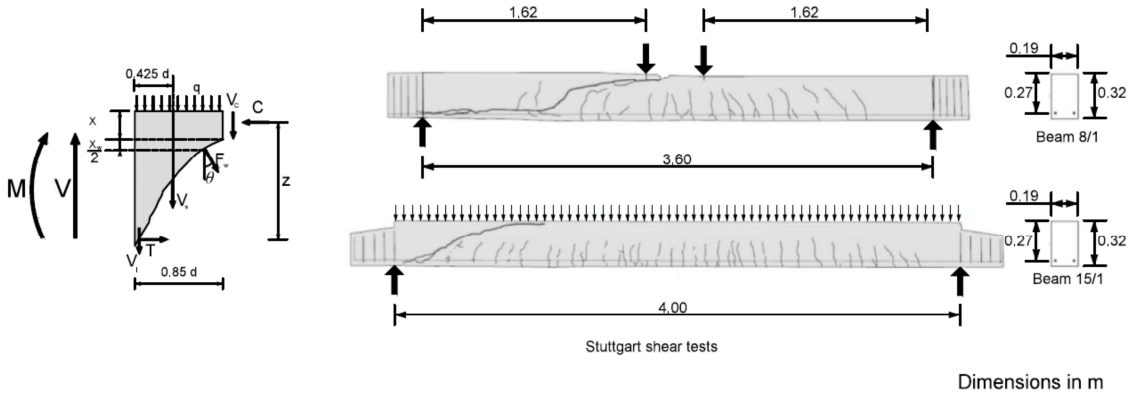

Figure 7. Beam subject to uniformly distributed loads. Shear forces and cracking pattern. Adapted from [27]

In relation to the shear span, *a*, for beams under uniformly distributed loads, the parameter that can be used in the calculation of the size effect, according to Eq. (8), is considered to be equal to $a=L/4$, being L the span of a simply supported beam or the distance between points with null bending moment.

5. COMPARISON WITH EXPERIMENTAL RESULTS

5.1 Database

Two databases published by Reineck et al. [12, 13] have been used to carry out a comparison of the proposal against experimental results and well-stablished code provisions. For beams without stirrups, the published databased comprises 744 tests with point loads and 40 tests with distributed loads. The only additional criterion used to filter the published database has been to only consider beams with rectangular cross-section, removing the T and I beams. Therefore, 720 tested beams without stirrups have been used, 680 with point loads and 40 with distributed loads. For elements with stirrups, 85 slender beams have been used from the 157 beams of the ACI-DAfStb large collection database for RC beams with stirrups [13], corresponding again to all beams

with rectangular cross-section. The range of the variables for the different tests is presented in Table 2.

	720 beams without stirrups		85 beams with stirrups	
	Min	**Max**	**Min**	**Max**
b (mm)	50	3005	125	457
d (mm)	65	3000	198	1200
f_{cm} (MPa)	13	139	16	125
ρ (%)	0.14	6.64	0.50	4.73
a/d	2.40	8.10	2.45	5.00
$A_{sw} \cdot f_{yw}$ (MPa)	-	-	0.32	3.07
V_{test} (kN)	7	1308	87	1172

Table 2 Range of variables in the employed databases

5.2 Code shear design formulation used for the comparison

The formulations given in Eurocode 2 [28], ACI 318-08 [29] and in Model Code 2010 [30] will be used to compare their predictions with the experimental results of the tests reported in the databases. All explicit partial safety factors have been removed from the original formulations. Moreover, the mean value of the materials strength has been used for all calculations, therefore, the predictions compared are not exactly the real predictions of the different models as f_{ck} or f'_c values should be used depending on the formulation employed.

For members without stirrups, the EC-2 procedure is an empirically derived method. However, for members with shear reinforcement, EC-2 formulation is based on a truss model with a variable angle of inclination of the struts and without any concrete contribution. For the calculation of the EC-2 prediction for members with stirrups the value considered has been the maximum between the prediction considering the stirrups (without concrete contribution) and the shear strength of an identical beam but without stirrups (no stirrup contribution).

The concrete contribution to the shear strength given by ACI 318-08 Code, which is also empirically based, has been calculated using its equation 11-5, both for elements with and without stirrups. For elements with stirrups, the ACI 318-08 formulation is based on a fixed 45° truss model with a concrete contribution identical to the shear strength of a identical beam but without stirrups.

The shear strength formulation in the Model Code 2010 is based on a "level of approximation" approach. On this paper, the level of approach with lower dispersion has been used to compare with the empirical results for elements with and without shear reinforcement. For this reason, for members without stirrups, the Level of Approximation II has been used; meanwhile the Level of Approximation III has been used when calculating the shear strength of members with stirrups. These two methods are directly based on the Modified Compression Field Theory [31]. Within this theory, the concrete contribution is predicted to be carried by aggregate interlock. The limits for the allowable angle of principal compression θ are also based on the MCFT. MC2010 presents a fourth level of approximation, which enables the use of tools such as nonlinear finite element analysis or generalized stress-field approaches [32]. This fourth level of approximation will not be considered in this paper because it is not a direct designing method. Note that the MC2010 shear provision is a structured approach that includes the design, detailed analysis and elaborate structural assessment of beams in shear [33].

5.3 Global comparison

A comparison of the performance of the new developed formulation with respect to the considered code formulations is given in Table 3 and Fig. 8. As can be seen, the proposed equation correlates better with the empirical results than any of the considered code formulations, few aspects will be signaled:

V_{test}/V_{pred}	720 beams without stirrups				85 beams with stirrups			
	EC-2	**ACI 318-08**	**MC10 Lev II**	**Proposal**	**EC-2**	**ACI 318-08**	**MC10 Lev III**	**Proposal**
Average	1.07	1.22	1.31	1.05	1.52	1.26	1.21	1.06
Median	1.03	1.22	1.27	1.02	1.53	1.25	1.22	1.06
Standard deviation	0.249	0.349	0.272	0.192	0.377	0.240	0.209	0.165
COV (%)	23.34	28.67	20.81	18.28	24.86	19.10	17.28	15.54
Minimum	0.40	0.26	0.51	0.54	0.53	0.68	0.75	0.65
$(V_{test}/V_{pred})_{5\%}$	0.75	0.64	0.97	0.81	0.91	0.90	0.92	0.83
Maximum	2.65	2.99	3.09	2.26	2.47	2.02	1.86	1.59
$(V_{test}/V_{pred})_{95\%}$	1.55	1.81	1.78	1.37	2.16	1.65	1.58	1.31

Table 3 Verification of the different shear design procedures

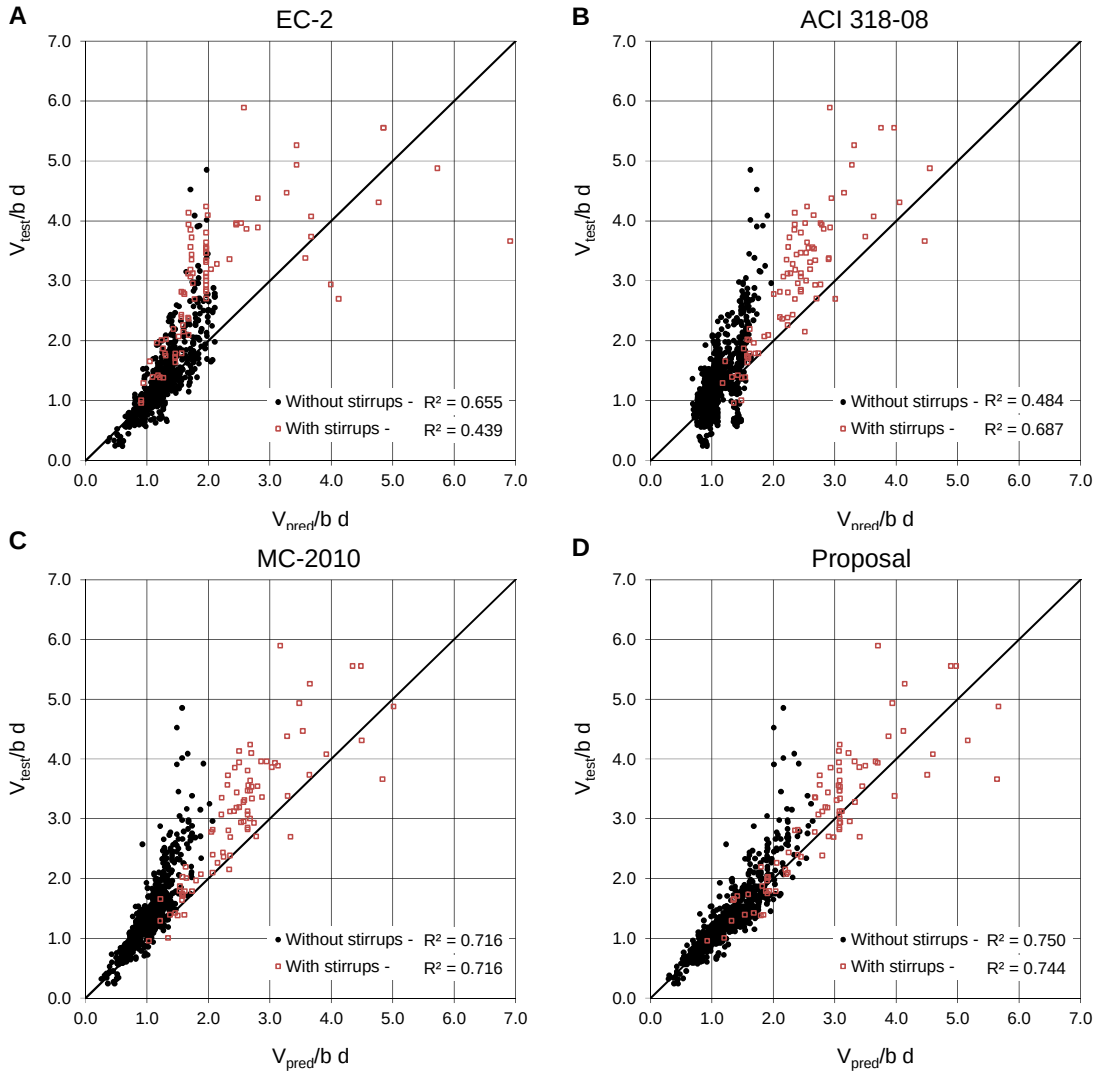

Figure 8. Correlation between the predictions and the experimental results

- The average of the V_{test}/V_{pred} ratio is directly related to accuracy; a value of 1.00 is highly accurate. The most accurate models among the different evaluated code procedures for elements without stirrups are EC2 (V_{test}/V_{pred} = 1.07) and the proposed new method (V_{test}/V_{pred} = 1.05). For elements with stirrups, the most accurate models are MC2010 – Level III (V_{test}/V_{pred} = 1.21) and the proposed new method (V_{test}/V_{pred} = 1.06). It must be highlighted that since code provisions should cover all possible cases within their respective scope, they are expected to be conservative.

- The standard deviation (SD) or the coefficient of variation (COV) is a measure of precision; the lower are the values, the higher is the precision. The most precise

models for elements without stirrups are the MC2010-Level II (COV = 20.81%) and the proposed method (COV = 18.28%). For elements with shear reinforcement, the most precise models are the MC2010-Level III (COV = 17.28%) and the proposed method (COV = 15.54%). The coefficient of determination, R^2, for each model is presented in Fig. 8.

- The 5% percentile of the V_{test}/V_{pred} ratio is a measure of safety of the formulation; although actual safety has to be assessed taking into account the load safety factors as well. Generally, a value close to 0.85 is considered to be the appropriate level of safety [34]; however, this value may vary with the codes. The MC-2010 is the safer procedure for both beams without ($V_{test}/V_{pred,\ 5\%} = 0.97$) and with shear reinforcement ($V_{test}/V_{pred,\ 5\%} = 0.92$). For the proposal, the 5% percentile equals to 0.81 for members without stirrups and 0.83 for members with stirrups. In any case, the calibration of the corresponding set of partial safety factors to be used in a semi-probabilistic format for shear design and assessment of the propose method is a pending task that would be able to calibrate the accuracy and safety of the method. In general terms, the needed level of conservatism depends on scatter and dispersion of the formulation with respect to observed experimentation, requiring larger safety factors for formulations with large scatter (lower precision).

The performance of the proposed model and the codes formulation in front of other databases may be seen elsewhere [1]. A simplified version of the proposed model has been also developed to predict the shear strength of concrete beams longitudinally reinforced with FRP bars. This simplified version has been validated with the results of 144 tested beams with very satisfactory results [17].

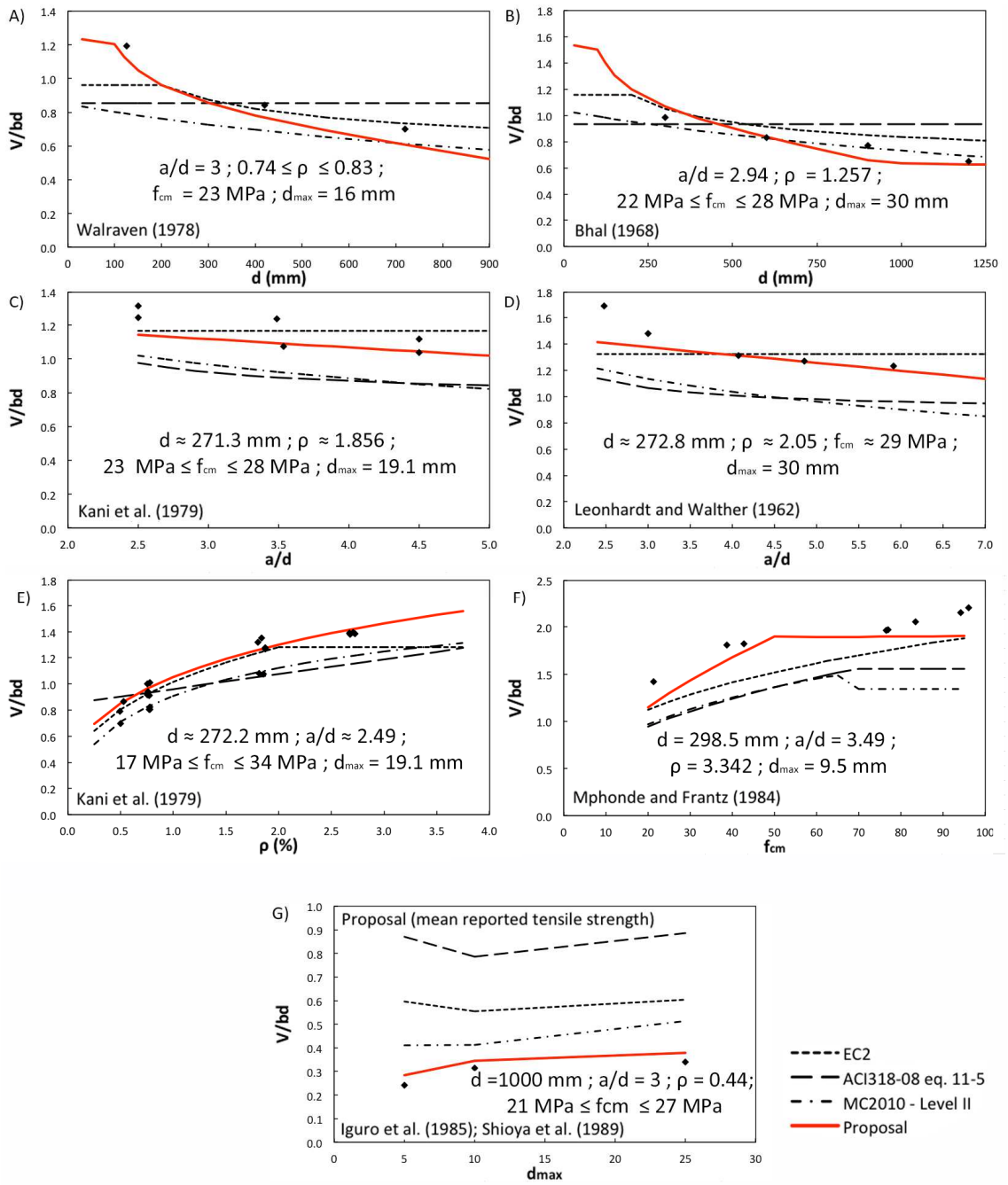

Figure 9. Correlation between the predictions and the experimental results of RC beams without shear reinforcement

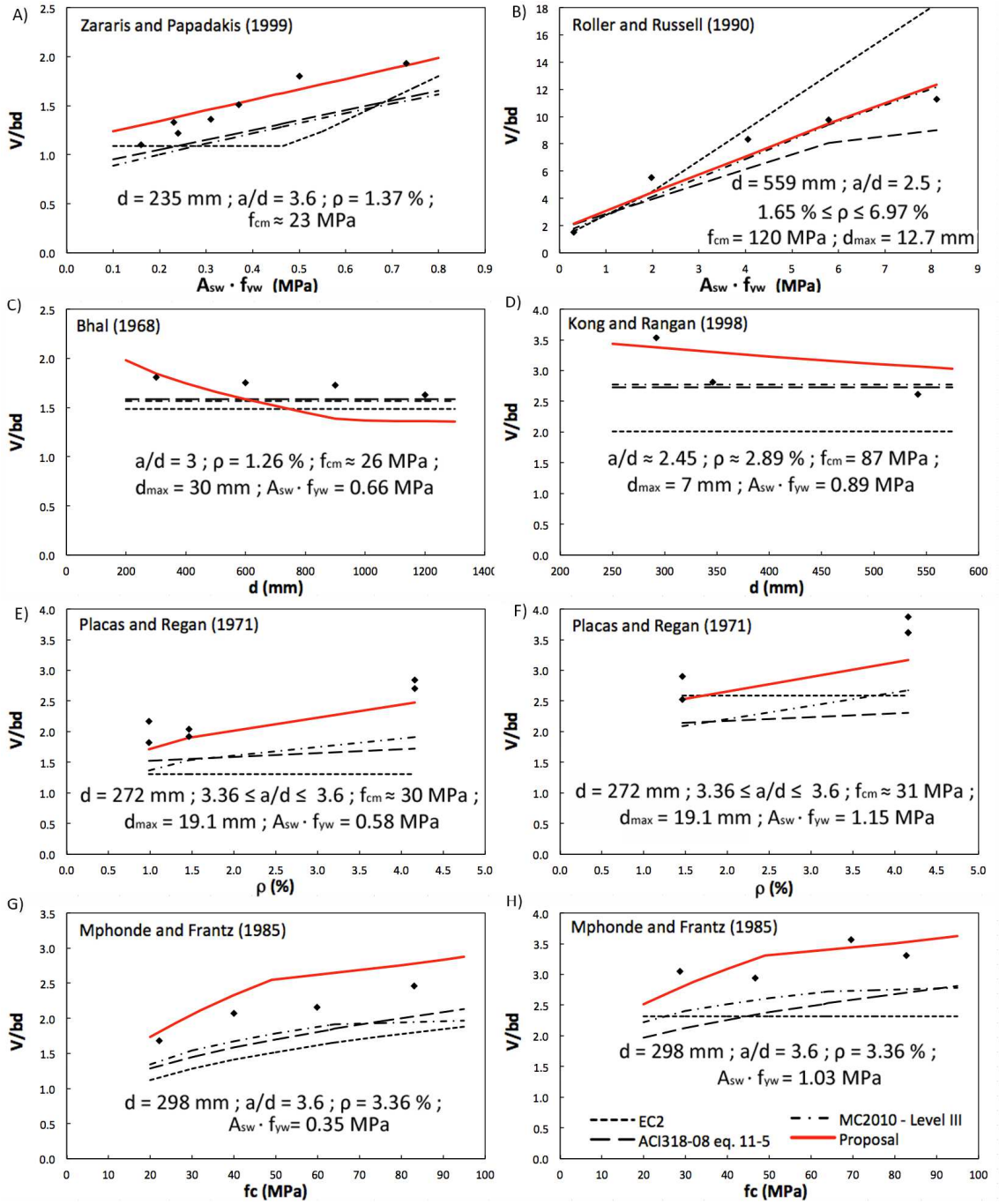

Figure 10. Correlation between the predictions and the experimental results of RC beams with shear reinforcement

5.4 Comparison with different series of tested beams

The predictions by the proposed formulation and the studied codes are compared in Figs. 9-10 with some selected series of tests from [27, 35-45]. The influence on the shear strength of the following design parameters is investigated: effective depth of the beam, d, shear-span-to-depth ratio, a/d, longitudinal reinforcement ratio, ρ, the mean compressive strength of concrete, f_{cm}, and the maximum aggregate size, d_{max}. Moreover,

for elements with stirrups, the influence of the mechanical amount of stirrups, $A_{sw} \cdot f_{yw}$, is also considered.

Figs. 9-10 provide a vast amount of information; however, few aspects will be signaled:

- The size effect, or the influence of the effective depth of the beam, is especially significant for elements without stirrups (Figs. 9A and 9B). However, for elements with stirrups, it may be also important as seen in the Kong and Rangan tests (Fig. 10D).

- The role of *a/d* is not taken into account in the EC2 formulation (Figs. 9C and 9D).

- The influence of the concrete compressive strength is taken into account in the proposed model indirectly, as the proposed formulation directly depends on the concrete tensile strength. For members without stirrups (Figure 9F) the tensile strength is limited to that corresponding to a concrete with a compressive strength to 60 MPa, as previously commented. This limitation is not used for elements with stirrups (Figs. 10G and 10H), although the relationship between the concrete compressive strength and the tensile strength changes for conventional concrete or high-strength concretes (Eqs. 9 and 10).

- The longitudinal reinforcement ratio, ρ, significantly influences the shear strength of beams with and without shear reinforcement (Figs. 9E, 10E and 10F). The EC2 formulation does not take into account its influence for beams with stirrups.

- The influence of the maximum aggregate size is taken into account in the shear transferred along the crack, being its influence lower than in the MC2010 formulation. In any case, the predictions of the tests by Iguro et al.(1985) and Shioya et al. (1989) in Fig. 9G show a very good correlation with the experimental results. Note that in this case, the reported tensile and compressive strength have been used for obtaining the predictions. The reported tensile strengths are significantly low in these tests.

- For elements with stirrups, the influence of the amount of shear reinforcement predicted by the proposed model (Figs. 10A and 10B) fits the experimental results

by Zararis and Papadakis (1999) and Roller and Russell (1990). The EC-2 model for members lightly shear reinforced would be very conservative if the shear strength of an identical beam but without was not considered.

The global comparison and the comparison with selected series of tests shows that empirical formulations (EC-2, ACI 318-08) present larger scatter and may neglect some important parameters, as was already commented by Muttoni and Fernández-Ruiz [46]. On the other hand, formulations based on mechanical models (i.e. MC2010 and the proposed formulation) give the best agreement when compared with experimental data, showing similar trends. These two models have been developed from different approaches, emphasizing the contribution of different shear transfer actions, and proposing different expressions with different governing parameters. Nevertheless, their strength predictions are similar and fit generally well with the experimental results. This fact suggests that successive mechanisms are activated as the load level increases and the structure becomes damaged, so that when equilibrium in a region is no longer possible with a governing shear transfer action, another action is activated. These redistributions of stresses may occur suddenly, given the brittle nature of cracking, but in some cases may produce small changes in the resultant internal forces, so that similar ultimate shear-flexural capacity can be obtained from different approaches.

6. APPLICATION EXAMPLE

Consider a simply supported beam in a 3-point bending configuration. Geometry and internal longitudinal and transverse reinforcement are shown in Fig. 11. The concrete compressive strength is 35 N/mm^2, the maximum aggregate size is 20 mm, and the steel reinforcement is B500S (f_{yw} = 500 N/mm^2). The design load acting at midspan is 550 kN. Previously to the resolution of this example, it should be mentioned that a safety factor calibration procedure is being under development by the time. Therefore, the design of the transversal steel reinforcement will be made without safety coefficients and assuming mean values of the concrete strength.

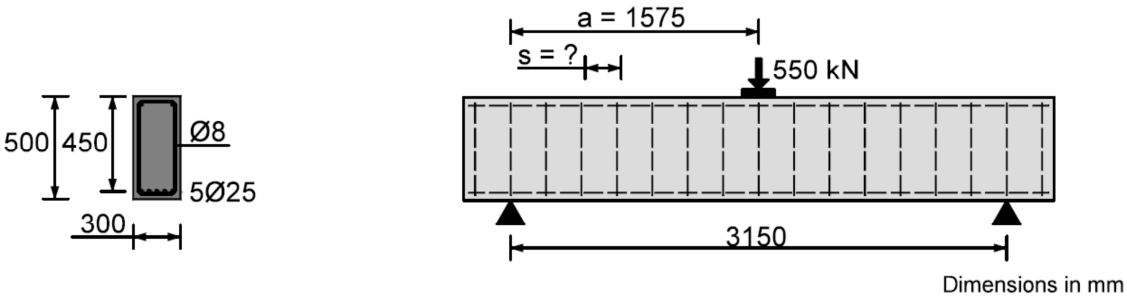

Figure 11. Beam geometry for the application example

The mechanical properties of the concrete needed to apply the model are: tensile strength, modulus of elasticity and fracture energy (Eqs. 9-12).

$$f_{ct.m} = 0.30\sqrt[3]{f_{ck}^2} = 0.30\sqrt[3]{35^2} = 3.21\ MPa$$

$$E_c = 22000\left(\frac{f_{cm}}{10}\right)^{0.3} = 22000\left(\frac{35}{10}\right)^{0.3} = 32036\ MPa$$

$$G_f = 0.028 \cdot f_{cm}^{0.18} \cdot d_{\max}^{0.32} = 0.028 \cdot 35^{0.18} \cdot 20^{0.32} = 0.138 N/mm$$

The longitudinal reinforcement amount and the modulus ratio are:

$$\rho = \frac{A_s}{b \cdot d} = \frac{2454}{300 \cdot 450} = 0.0182$$

$$\alpha_e = \frac{E_s}{E_c} = \frac{200}{32.04} = 6.24$$

The neutral axis depth, calculated with a linear concrete stress distribution (Eq. 2) is:

$$\xi = \frac{x}{d} = \alpha_e \cdot \rho \cdot \left(-1 + \sqrt{1 + \frac{2}{\alpha_e \cdot \rho}}\right) = 0.376$$

The size effect factor (Eq. 8) is:

$$\zeta = 1.2 - 0.2 \cdot a = 1.2 - 0.2 \cdot 1.575 = 0.885 \geq 0.65$$

The dimensionless design shear force is equal to:

$$v_{Sd} = \frac{V_{Sd}}{f_{ct} \cdot b \cdot d} = \frac{275000}{3.21 \cdot 300 \cdot 450} = 0.635$$

The dimensionless shear strength resisted along the crack and by the concrete compression chord (considering the beam without shear reinforcement) can be obtained from Eqs. (4) and (7), respectively. In this case of beam without stirrups, the shear contribution of the longitudinal reinforcement (dowel action) is negligible (Eq. 5b).

$$v_w = 167 \frac{f_{ct}}{E_c}\left(1 + \frac{2E_c G_f}{{f_{ct}}^2 d}\right) = 167 \frac{3.21}{32036}\left(1 + \frac{2 \cdot 32036 \cdot 0.138}{3.21^2 \cdot 450}\right) = 0.049$$

$$v_c = \zeta\left[\left(0.88 + 0.70 \cdot v_s\right) \cdot \frac{x}{d} + 0.02\right] = 0.885\left[\left(0.88 + 0.70 \cdot 0\right) \cdot 0.376 + 0.02\right] = 0.311$$

Therefore, the total shear force resisted without considering the transversal reinforcement (Eqs.19-20) equals to:

$$v_{u,0} = v_c + v_w = 0.311 + 0.049 = 0.36$$

$$V_{u,0} = f_{ct} \cdot b \cdot d \cdot \left(v_c + v_w\right) = 3.21 \cdot 300 \cdot 450 \cdot \left(0.311 + 0.049\right) = 155.7\ kN$$

Since the design shear force is higher than the shear force resisted by the beam without stirrups it is necessary to add transversal steel reinforcement. Equation (21) provides the amount of transversal reinforcement. Previously, the shear contribution of the longitudinal reinforcement (dowel action) is estimated by means of Eq. (5a).

$$v_l \simeq 0.25 \cdot \xi - 0.05 = 0.25 \cdot 0.376 - 0.05 = 0.044$$

$$v_s = \frac{v_{Sd} - \left(v_{u,0} + v_l\right)}{1 + 0.70 \cdot \zeta \cdot \frac{x}{d}} = \frac{0.635 - \left(0.36 + 0.044\right)}{1 + 0.70 \cdot 0.885 \cdot 0.376} = 0.188$$

From the dimensionless transversal steel contribution it is possible to obtain the amount of needed transversal steel reinforcement through Eq. (6).

$$v_s = 0.188 = 0.85\rho_w \frac{f_{yw}}{f_{ct}} = 0.85\rho_w \frac{500}{3.21} \qquad \rho_w = 1.42 \cdot 10^{-3}$$

Therefore, the exact result from the calculation provides closed stirrups ϕ8@236 mm. According to the EC2, without applying safety coefficients, it is necessary closed stirrups ϕ8@185 mm.

In the following lines, a strength verification will be performed considering the same beam as in the previous design example but with transverse reinforcement that consists on closed stirrups ϕ8@200 mm (ρ_w =1.68·10^{-3}).

The shear resisted by the stirrups is given by Eq. (6):

$$v_s = 0.85\rho_w \frac{f_{yw}}{f_{ct}} = 0.85 \cdot 1.68 \cdot 10^{-3} \frac{500}{3.21} = 0.222$$

$$V_s = v_s f_{ct} \cdot b \cdot d = 0.222 \cdot 3.21 \cdot 300 \cdot 450 = 96.13\ kN$$

The shear resisted by the concrete chord (Eq. 7) is:

$$v_c = \zeta \left[(0.88 + 0.70v_s)\frac{x}{d} + 0.02\right] = 0.885[(0.88 + 0.7 \cdot 0.222)0.376 + 0.02] = 0.362$$

$$V_c = v_c f_{ct} \cdot b \cdot d = 0.362 \cdot 3.21 \cdot 300 \cdot 450 = 156.87\ kN$$

The shear resisted along the crack can be calculated as (Eq. 4):

$$v_w = 167\frac{f_{ct}}{E_c}\left(1 + \frac{2E_c G_f}{{f_{ct}}^2 d}\right) = 167\frac{3.21}{32036}\left(1 + \frac{2 \cdot 32036 \cdot 0.138}{3.21^2 \cdot 450}\right) = 0.049$$

$$V_w = v_w f_{ct} \cdot b \cdot d = 0.049 \cdot 3.21 \cdot 300 \cdot 450 = 21.23\ kN$$

The shear resisted by the longitudinal reinforcement is given by Eq. (5a):

$$v_l \simeq 0.25 \cdot \xi - 0.05 = 0.25 \cdot 0.376 - 0.05 = 0.044$$

$$V_l = v_l f_{ct} \cdot b \cdot d = 0.044 \cdot 3.21 \cdot 300 \cdot 450 = 19.07\ kN$$

And the total shear resisted (Eq. 1) is:

$$V = V_c + V_w + V_l + V_s = 293.3\ kN$$

Therefore, since the design shear force is lower than the ultimate shear force, the beam shear-flexural strength is satisfactory.

The cracking moment is M_{cr} = 49.87 kN·m when considering the amount of longitudinal reinforcement. This bending moment is reached at a distance from the support s_{cr} = M_{cr}/V_u= 49.87/293.3 = 0.17 m, which equals 0.378 *d*. The distance from the critical section to the support (Fig. 3) is $s_u = s_{cr}$ +0.85*d* = 0.17 + 0.85·0.45 = 0.552 m, and the bending moment at the shear critical section is $M = V_u$·0.552 = 161.90 kN·m. The first branch of the critical shear crack forms an angle with the longitudinal axis of 36.27º (Eq. 3), the inclination of the second branch with the longitudinal axis is 9.42º (obtained geometrically from Fig. 3 and the results of this example). Moreover, it will be possible to obtain the normal stresses at the critical section at the point of the compressive chord where failure occurs, the shear stress also at the critical point, the principal stresses and to verify that the principal stresses satisfy Kupfer's failure envelope. See reference [1] for further detail of the needed equations.

7. CONCLUSIONS

A mechanical model for the shear strength of slender reinforced concrete beams with and without shear reinforcement has been presented. It considers that the shear strength is the sum of the shear transferred by the concrete compression chord, along the crack, due to residual tensile and frictional stresses, by the stirrups and, if they exist, by the longitudinal reinforcement. The following conclusions can be drawn:

- The proposed expressions provide qualitative and quantitative information about the parameters that govern the structural behavior, which is very useful for the design or for the assessment of existing structures. Moreover, the formulation is valid for designing and checking without iterations.

- The shear transferred by the concrete compression chord is a fundamental contribution in this model. It has been found that this contribution is linearly dependent on the relative flexural neutral axis depth, *x/d*, which is a function of $\alpha_e \cdot \rho$, being $\alpha_e = E_s/E_c$ the modular ratio and $\rho = A_s/(b \cdot d)$ the longitudinal reinforcement ratio.

- The model has been extended for beams subjected to uniformly distributed loads. Due to the mechanical nature of the model, the extension has been carried out just adding a new term in the equilibrium equations. However, this new term is negligible, and the concrete chord contribution of beams with uniformly distributed loads can be considered equal to that obtained in the case of point loads. Nonetheless, the position of the critical shear crack and the critical section is closer to the support than in the case of beams subjected to point loads.

- The predictions of the present model fit very well the experimental results of rectangular beams collected in the new ACI-DAfStb databases of shear tests on slender reinforced concrete beams with and without stirrups. The mean value (MV) and the coefficient of variation (COV) of the ratio between the predicted and the experimentally measured shear strength obtained are MV=1.05, COV =18.28% for beams without stirrups and MV=1.06, COV=15.54% for beams with stirrups. These results present a better approximation and less scatter than those obtained by using the EC2, MC2010 and ACI 318-08 provisions. This is relevant, given the simplicity of the expressions derived, avoiding unjustified oversizing for the design of new structures. In addition, if the proposed formulation is used for the assessment of existing structures, they could avoid unnecessary structural reinforcements since the real strength of the structure could be higher than reflected by current concrete codes.

The mechanical nature of the model allows adapting it to different cases, such as continuous beams, T- or I-sections, partially prestressed beams or with moderate axial loads, etc. For beams with T- or I-sections, for instance, the contribution of the concrete compression chord may be very important, as opposed to what is considered by most existing codes. Finally, it's important to highlight that a calibration of the corresponding set of partial safety factors to be used in a semi-probabilistic format for shear design and assessment is needed.

ACKNOWLEGEMENTS

This work has been developed under the framework of the Research Projects "BIA2012-31432" and "BIA2012-36848", both funded by the Spanish Ministry of

Economy and Competitiveness (MINECO) and co-funded by the European Regional Development Funds (ERDF).

REFERENCES

[1] Marí A, Bairán JM, Cladera A, Oller E, Ribas C. Shear-flexural strength mechanical model for the design and assessment of reinforced concrete beams. Struct Infrastruct E 2014;DOI: 10.1080/15732479.2014.964735.

[2] Petrangeli M, Pinto PE, Ciampi V. Fiber element for cyclic bending and shear of RC structures. I: Theory. J Eng Mech 1999;125:994-1001.

[3] Bentz EC. Sectional analysis of reinforced concrete members. Doctoral dissertation, University of Toronto 2000:184.

[4] Bairán JM, Marí AR. Coupled model for the non-linear analysis of anisotropic sections subjected to general 3D loading. Part 1: Theoretical formulation. Comput Struct 2006;84:2254-63.

[5] Navarro-Gregori J, Miguel-Sosa P, Fernández-Prada MA, Filippou FC. A 3D numerical model for reinforced and prestressed concrete elements subjected to combined axial, bending, shear and torsion loading. Eng Struct 2007;29:3404-19.

[6] Saritas A, Filippou FC. Inelastic axial-flexure-shear coupling in a mixed formulation beam finite element. Int J Non Linear Mech 2009;44:913-22.

[7] Mohr S, Bairán JM, Marí AR. A frame element model for the analysis of reinforced concrete structures under shear and bending. Eng Struct 2010;32:3936-54.

[8] Ferreira D, Bairán J, Marí A. Numerical simulation of shear-strengthened RC beams. Eng Struct 2013;46:359-74.

[9] Nielsen M, Hoang L. Limit analysis and concrete plasticity, Boca Raton - Florida: CRC Press, 1999.

[10] Recupero A, D'Aveni A, Ghersi A. N-M-V interaction domains for box and I-shaped reinforced concrete members. ACI Struct J 2003;100:113-9.

[11] Bairán JM, Marí AR. Multiaxial-coupled analysis of RC cross-sections subjected to combined forces. Eng Struct 2007;29:1722-38.

[12] Reineck K-, Bentz EC, Fitik B, Kuchma DA, Bayrak O. ACI-DAfStb database of shear tests on slender reinforced concrete beams without stirrups. ACI Struct J 2013;110:867-75.

[13] Reineck K, Bentz E, Fitik B, Kuchma DA, Bayrak O. ACI-DAfStb Databases for Shear Tests on Slender Reinforced Concrete Beams with Stirrups. ACI Struct J 2014;111.

[14] Cladera A, Marí AR. Shear design procedure for reinforced normal and high-strength concrete beams using artificial neural networks. Part I: Beams without stirrups. Eng Struct 2004;26:917-26.

[15] Cladera A, Marí AR. Shear design procedure for reinforced normal and high-strength concrete beams using artificial neural networks. Part II: Beams with stirrups. Eng Struct 2004;26:927-36.

[16] Cladera A, Marí AR. Experimental study on high-strength concrete beams failing in shear. Eng Struct 2005;27:1519-27.

[17] Marí A, Cladera A, Oller E, Bairán J. Shear design of FRP reinforced concrete beams without transverse reinforcement. Compos Part B: Eng 2014;57:228-41.

[18] Karayannis CG, Chalioris CE. Shear tests of reinforced concrete beams with continuous rectangular spiral reinforcement. Constr Build Mater 2013;46:86-97.

[19] Collins MP, Bentz EC, Sherwood EG, Xie L. An adequate theory for the shear strength of reinforced concrete structures. Magazine of Concrete Research 2008;60:635-50.

[20] Kupfer HB, Gerstle KH. Behavior of concrete under biaxial stresses. Journal of the Engineering Mechanics Division 1973;99:853-66.

[21] Arezoumandi M, Volz JS. Effect of fly ash replacement level on the fracture behavior of concrete. Frontiers of Structural and Civil Engineering 2013;7:411-8.

[22] Arezoumandi M, Ezzell M, Volz JS. A comparative study of the mechanical properties, fracture behavior, creep, and shrinkage of chemically based self-consolidating concrete. Frontiers of Structural and Civil Engineering 2014;8:36-45.

[23] Zhang XX, Abd Elazim AM, Ruiz G, Yu RC. Fracture behaviour of steel fibre-reinforced concrete at a wide range of loading rates. Int J Impact Eng 2014;71:89-96.

[24] Zararis PD, Papadakis GC. Diagonal shear failure and size effect in RC beams without web reinforcement. J Struct Eng 2001;127:733-42.

[25] Tureyen AK, Frosch RJ. Concrete Shear Strength: Another Perspective. ACI Struct J 2003;100:609-15.

[26] Cladera A, Marí AR. Shear design of prestressed and reinforced concrete beams. Mag Concr Res 2006;58:713-22.

[27] Leonhardt F, Walther R. Schubversuche an Einfeldrigen Stahlbeton-Balken mit und ohne Schubbewehrung zur Ermittlung der Schubtragfhigkeit und der Oberen Schubspannungsgrenze. Heft 151, Deutcher Ausschuss Fr Stahlbeton 1962:66.

[28] European Committee for Standardization (CEN). Eurocode 2: Design of Concrete Structures: Part 1: General Rules and Rules for Buildings: European Committee for Standardization, 2002.

[29] ACI Committee 318. Building Code Requirements for Structural Concrete (ACI 318-08) and Commentary, Farmington Hills, MI, USA: American Concrete Institute, 2008.

[30] Féderation International du Beton. Model Code 2010, Final Draft: Féderation International du Beton, 2012.

[31] Vecchio FJ, Collins MP. The modified compression-field theory for reinforced concrete elements subjected to shear. ACI J. 1986;83:219-31.

[32] Bentz E. MC2010: Shear strength of beams and implications of the new approaches. Workshop “RecentDevelopments on Shear and Punching Shear in RC and FRC Elements” 2010;fib Bulletin 57:15-30.

[33] Sigrist V, Hackbarth B. A structured approach to the design and analysis of beams in shear 2010;57:93-104.

[34] Collins M. Evaluation of shear design procedures for concrete structures. Report prepared for the CSA Technical Committee on Reinforced Concrete Design, Ottawa, Canada 2001.

[35] Walraven JC. The influence of depth on the shear strength of lightweight concrete beams without shear reinforcement. Stevin Lab , Delft Univ 1978;Report S-78-4.

[36] Bhal NS. Uber den Einfluss der Balkenhöhe auf Schubtragfähigkeit von einfeldrigen Stahlbetonbalken mit und ohne Schubbewehrung. Über den Einfluss der Balkenhöhe auf Schubtragfähigkeit von Einfeldrigen Stahlbetonbalken mit und Ohne Schubbewehrung 1968:124.

[37] Kani MW, Huggins MW, Wittkopp RR. Kani on shear in reinforced concrete: Dept. of Civil Engineering, University of Toronto, 1979.

[38] Mphonde AG, Frantz GC. Shear tests of high-and low-strength concrete beams without stirrups. ACI-Journ 1984;81:350-7.

[39] Iguro M, Shioya T, Nojiri Y, Akiyama H. Experimental studies on shear strength of large reinforced concrete beams under uniformly distributed load. Concrete Library International of JSCE 1985;5:137-46.

[40] Shioya T, Iguro M, Nojiri Y, Akiyama H, Okada T. Shear strength of large reinforced concrete beams. Fracture Mechanics: Application to Concrete 1989;118:259-79.

[41] Zararis PD, Papadakis G. Influence of the arrangement of reinforcement on the shear strength of RC beams. Proceedings of the 13th Hellenic Conference on Concrete 1999;1:110-9.

[42] Roller JJ, Russell HG. Shear strength of high-strength concrete beams with web reinforcement. ACI Struct J 1990;87:191-8.

[43] Kong PYL, Rangan BV. Shear strength of high-performance concrete beams. ACI Struct J 1998;95:677-88.

[44] Placas A, Regan PE. Shear failure of reinforced concrete beams. J Amer Concrete Inst 1971;68:763-73.

[45] Mphonde AG, Frantz GC. Shear tests of high- and low-strength concrete beams with stirrups. High-Strength Concrete 1985:179-96.

[46] Muttoni A, Ruiz MF. Shear strength of members without transverse reinforcement as function of critical shear crack width. ACI Struct J 2008;105:163-72.